Inactivation of rice starch branching enzyme IIb triggers broad and unexpected changes in metabolism by transcriptional reprogramming

Can Baysal[a], Wenshu He[a], Margit Drapal[b], Gemma Villorbina[c], Vicente Medina[a], Teresa Capell[a], Gurdev S. Khush[d,1], Changfu Zhu[a], Paul D. Fraser[b], and Paul Christou[a,e,1]

[a]Department of Plant Production and Forestry Science, University of Lleida-Agrotecnio Center, 25198 Lleida, Spain; [b]Department of Biological Sciences, Royal Holloway University of London, TW20 0EX Egham, United Kingdom; [c]Department of Chemistry, University of Lleida-Agrotecnio Center, 25198 Lleida, Spain; [d]Department of Plant Sciences, University of California, Davis, CA 95616; and [e]Catalan Institute for Research and Advanced Studies (ICREA), 08010 Barcelona, Spain

Contributed by Gurdev S. Khush, August 26, 2020 (sent for review July 15, 2020; reviewed by Fredy Altpeter and Keerti S. Rathore)

Starch properties can be modified by mutating genes responsible for the synthesis of amylose and amylopectin in the endosperm. However, little is known about the effects of such targeted modifications on the overall starch biosynthesis pathway and broader metabolism. Here we investigated the effects of mutating the *OsSBEIIb* gene encoding starch branching enzyme IIb, which is required for amylopectin synthesis in the endosperm. As anticipated, homozygous mutant plants, in which OsSBEIIb was completely inactivated by abolishing the catalytic center and C-terminal regulatory domain, produced opaque seeds with depleted starch reserves. Amylose content in the mutant increased from 19.6 to 27.4% and resistant starch (RS) content increased from 0.2 to 17.2%. Many genes encoding isoforms of AGPase, soluble starch synthase, and other starch branching enzymes were up-regulated, either in their native tissues or in an ectopic manner, whereas genes encoding granule-bound starch synthase, debranching enzymes, pullulanase, and starch phosphorylases were largely down-regulated. There was a general increase in the accumulation of sugars, fatty acids, amino acids, and phytosterols in the mutant endosperm, suggesting that intermediates in the starch biosynthesis pathway increased flux through spillover pathways causing a profound impact on the accumulation of multiple primary and secondary metabolites. Our results provide insights into the broader implications of perturbing starch metabolism in rice endosperm and its impact on the whole plant, which will make it easier to predict the effect of metabolic engineering in cereals for nutritional improvement or the production of valuable metabolites.

endosperm | high-amylose rice | metabolomics | starch biosynthesis | transcriptomics

Starch is the major storage polysaccharide in higher plants. It is a mixture of linear amylose, in which glucose residues are linked by α(1 → 4) glycosidic bonds, and amylopectin, in which amylose-like chains feature additional branches formed by α(1 → 6) glycosidic bonds every 24 to 30 glucose units. Rice starch typically consists of ∼20% amylose and ∼80% amylopectin (1, 2). Amylose synthesis requires only two enzymes: ADP-glucose pyrophosphorylase (AGPase) and granule-bound starch synthase (GBSS). In contrast, the synthesis of amylopectin involves the combined activity of AGPase, soluble starch synthases (SSs), starch branching enzymes (SBEs), debranching enzymes (DBEs), pullulanase (PUL), and phosphorylases (Phos), the latter forming a complex with disproportionating enzyme (3, 4). The rice genome encodes seven AGPase subunits, 10 isoforms of SSs, 3 isoforms of SBEs, 4 isoforms of DBEs, and 2 isoforms of Phos, with different expression profiles and activities, underpinning the complex regulation of starch metabolism in this species (5).

SBE is the only enzyme that introduces α(1 → 6) glycosidic bonds into α-polyglucans, and it is therefore essential for amylopectin biosynthesis (6). The three isoforms in rice (OsSBEI, OsSBEIIa, and OsSBEIIb) play distinct roles, with OsSBEI favoring predominantly linear amylose-like substrates and the others favoring amylopectin substrates and thus acting to increase the density of branching (7, 8). OsSBEIIb is the major isozyme found in rice seeds due to the strong endosperm-specific expression profile of the *OsSBEIIb* gene. OsSBEIIb also has the unique ability to transfer short chains to the crystalline lamellae of amylopectin, whereas OsSBEIIa lacks this function (6, 9). *OsSBEIIa* is expressed in all rice tissues including the developing endosperm and is the major isoform found in leaves (5).

The inactivation of OsSBEI and/or OsSBEIIa does not affect seed morphology in rice (10–12), whereas the inactivation of OsSBEIIb generates *amylose extender* (*ae*) mutants containing starch molecules with longer amylopectin chains and fewer branches, increasing the amylose content and producing an opaque seed phenotype (9, 11, 13). In rice cultivar Kinmaze, the *ae* mutation was shown to reduce the dry seed weight by 35% compared to wild-type plants and to increase the amylose content of the seeds from 15.7 to 26.5% (9).

The inactivation of individual starch biosynthesis enzymes in rice can have a wider effect on general starch metabolism, causing the modulation of genes encoding other enzymes in the pathway (9, 13). Interestingly, even when the target gene is endosperm

Significance

The properties of starch can be modified by manipulating enzymes that extend the polymer backbone, add new branches, or remove them. The effects of such interventions on wider metabolism are rarely investigated but could help to predict the best metabolic engineering strategies. We mutated the rice gene *OsSBEIIb* encoding starch branching enzyme IIb, which is required for the synthesis of densely branched amylopectin in the endosperm. We investigated the effect on starch properties, seed morphology, and the expression of starch biosynthesis genes in the endosperm and leaf, observing broad transcriptional reprogramming. The mutation also had a wide effect on general primary and secondary metabolism in the endosperm, causing the accumulation of sugars, fatty acids, amino acids, and phytosterols.

Author contributions: C.B., G.S.K., and P.C. designed research; C.B., W.H., M.D., V.M., T.C., and C.Z. performed research; C.B., W.H., M.D., G.V., T.C., G.S.K., C.Z., P.D.F., and P.C. analyzed data; and C.B., G.S.K., and P.C. wrote the paper.

Reviewers: F.A., University of Florida; and K.S.R., Texas A&M University.

The authors declare no competing interest.

[1]To whom correspondence may be addressed. Email: gurdev@khush.org or paul.christou@udl.cat.

This article contains supporting information online at https://www.pnas.org/lookup/suppl/doi:10.1073/pnas.2014860117/-/DCSupplemental.

First published October 5, 2020.

specific, the ripple effects can be evident in vegetative tissues, as shown for *OsGBSSI* (14) and *OsAPL2*, encoding the large subunit of cytosolic AGPase (15). This may reflect the accumulation of intermediates that trigger feedback inhibition and/or the effect of enzyme depletion or structural disruption on the activity of metabolons (enzyme consortia that function as supramolecular complexes) (2, 16). The broader effects of metabolic interventions can be determined by comparing wild-type and mutant plants at the transcriptomic and metabolomic levels (17, 18), but this form of systematic analysis is rarely carried out and therefore the broader implications of perturbing starch metabolism in the endosperm and its impact on the whole plant are unclear.

Here we evaluated the wider impact of mutating *OsSBEIIb* by analyzing the starch biosynthesis transcriptome and broader metabolome of a mutant line generated using the CRISPR/Cas9 system, which has a phenotype similar to the original *ae* mutant (19). We investigated the effect of the mutation on the structure and function of the OsSBEIIb protein, on the morphology of starch granules in the mutant endosperm, and on the properties of the extracted starch. We also analyzed the expression of a panel of 26 genes related to starch biosynthesis in the endosperm and leaves and measured the abundance of diverse primary and secondary metabolites in the endosperm in order to determine how the inactivation of OsSBEIIb might affect overall carbohydrate metabolism, as well as primary and secondary metabolism more broadly.

Results

The Mutation Site in *OsSBEIIb* Abolishes the Catalytic Center of the Enzyme. The *OsSBEIIb* gene was targeted by using the CRISPR/Cas9 system to introduce a double-strand break in exon 12, resulting in a 4-bp deletion that generated a frameshift and premature stop codon (19). T0 transformants heterozygous for the mutant allele were self-pollinated over two generations to yield homozygous T2 progeny lacking the *cas9* transgene. We used this line (E15) to investigate changes at the protein level that might explain the loss of OsSBEIIb activity. We translated the mutant sequence and aligned it with wild-type OsSBEIIb (*SI Appendix*, Fig. S1*A*) allowing us to identify key functional residues (*SI Appendix*, Fig. S1*B*). Homology modeling was then used to determine the effect of the mutation on the structure and key functional residues of the enzyme (Fig. 1).

The catalytic domains of SBEs are highly conserved in plants (4, 20). Seven amino acids in the maize ortholog ZmSBEIIb are necessary for catalysis (Asp^{376}, His^{381}, Arg^{445}, Asp^{447}, Glu^{502}, His^{569}, and Asp^{570}) in addition to the catalytic triad (Asp^{447}, Glu^{502}, and Asp^{570}) which was previously shown to reside in the central domain (4). The corresponding amino acids in the OsSBEIIb protein are Asp^{402}, His^{407}, Arg^{471}, Asp^{473}, Glu^{528}, His^{595}, and Asp^{596}, supporting the catalytic triad Asp^{473}, Glu^{528}, and Asp^{596}, indicating that the two sequences are offset by 26 residues (*SI Appendix*, Fig. S1*B*). The 4-bp deletion in line E15 occurred immediately downstream of Gly^{418} and the frameshift generated a new sequence of 31 amino acids followed by a termination codon (*SI Appendix*, Fig. S1*A*).

The comparative models of wild-type OsSBEIIb and the mutant version revealed that the deletion and frameshift caused the complete loss of the catalytic triad (*SI Appendix*, Fig. S2) as well as the Arg^{471} residue that plays a key role in stabilizing the catalytic center (Fig. 1 *A* and *B*). The E15 mutant retains only residues Asp^{402} and His^{407} of the central catalytic domain and these are insufficient to stabilize the enzyme structure (Fig. 1*B*). The loss of OsSBEIIb activity in line E15 therefore reflects the disruption of the catalytic center and loss of the regulatory C-terminal domain that determines substrate specificity.

Loss of OsSBEIIb Activity Alters the Starch Grain Content and Structure. The endosperm amylose content of the T3 seeds in line E15 was 27.4%, 1.4-fold higher than that of wild-type seeds (19.6%) and a Tos17 insertion line (NE9005) with the transposon integrated into intron 18 of the *OsSBEIIb* gene (19.5%). The mutation also substantially increased the resistant starch content from 0.2% in wild-type and NE9005 seeds to 17.2% in line E15 (Fig. 2*A* and *SI Appendix*, Fig. S3). However, the total starch content was ~26% lower in line E15, resulting in significantly smaller seeds with lower dry seed and dehulled grain weights. The dry weight of the E15 seeds was 14.7 ± 1.9 mg (compared to 24.9 ± 2.8 mg for wild-type seeds) and the dehulled grain weight was 13.1 ± 1.4 mg (compared to 18.2 ± 2.4 mg for wild-type seeds) (*SI Appendix*, Table S1).

Morphological analysis by light microscopy revealed that the E15 grains were opaque, whereas those of the wild-type and NE9005 lines were uniformly translucent (Fig. 2 *B*, *i–vi*). Scanning electron microscopy revealed that the loss of OsSBEIIb activity had a profound influence on the structure of starch grains. In wild-type lines, the starch grains were homogeneous, compact, and angular, with few interstitial spaces, whereas those in the E15 mutant varied considerably in size, were rounded rather than angular, and separated by large gaps (Fig. 2 *B*, *vii–ix*).

Loss of OsSBEIIb Activity Causes the Broad Transcriptional Reprogramming of Starch Metabolism. To determine whether the loss of OsSBEIIb activity caused a ripple effect on starch metabolism, we compared the expression profiles of 26 genes involved in starch biosynthesis representing five classes of enzymes (AGPase, SS, SBE, DBE, and Pho). We carried out a separate analysis of the isoforms expressed specifically in the endosperm 15 d after fertilization (DAF) and those expressed in the leaves at the same time. Heat maps comparing the expression of these genes in the endosperm and leaves are shown in Fig. 3*A*.

Rice AGPase is a tetramer of two large subunits and two small subunits. There are four large subunit genes (*OsAGPL1–4*) and two small subunit genes (*OsAGPS1* and *OsAGPS2*, the latter producing mRNA variants *OsAGPS2a* and *OsAGPS2b* by alternative splicing). Some of them are predominantly expressed in the endosperm (e.g., *OsAGPL2* and *OsAGPS2b*) while others are predominantly expressed in the leaves (e.g., *OsAGPS2a* and *OsAGPL3*) (5). We found that *OsAGPL1* and *OsAGPS1* were minimally expressed in the endosperm and leaves of both genotypes. *OsAGPS2a* was expressed at low levels in the leaves but was 1.5-fold higher in the E15 line than wild-type plants. *OsAGPS2b* was strongly expressed in the seeds and was 2-fold higher in the E15 line than wild-type plants. *OsAGPL2* was expressed more strongly in the endosperm than leaves of wild-type plants and there was a slight but statistically nonsignificant increase in the endosperm of line E15 but a striking 1.7-fold increase in the leaves. *OsAGPL3* was predominantly expressed in the leaves of wild-type plants, but we observed a significant increase in expression in both the leaves (1.7-fold) and endosperm (1.6-fold) in line E15. *OsAGPL4* expression was not detected in either tissue.

We also observed a major transcriptional reprogramming of genes encoding starch synthases. *OsSSI* was strongly expressed in the developing endosperm and leaves of wild-type plants and was up-regulated in both tissues in line E15, although the change was only statistically significant (2.2-fold) in the endosperm. *OsSSIIa* was only expressed in the endosperm and was significantly (1.6-fold) up-regulated in line E15. *OsSSIIb* was only expressed in the leaves of wild-type plants and a similar (1.6-fold) up-regulation was observed in the mutant. *OsSSIIc* was expressed in both tissues and we observed a significant (1.8-fold) increase in the E15 leaf tissue but no change in the endosperm. *OsSSIIIa* is endosperm specific and there was no significant difference between wild-type and E15 seeds. *OsSSIIIb*, *OsSSIVa*, and *OsSSIVb* are expressed in both tissues but the only change we observed was in the leaf, where the expression levels of all three genes increased by 1.6-fold in the mutant. Finally, the endosperm-specific *OsGBSSI*

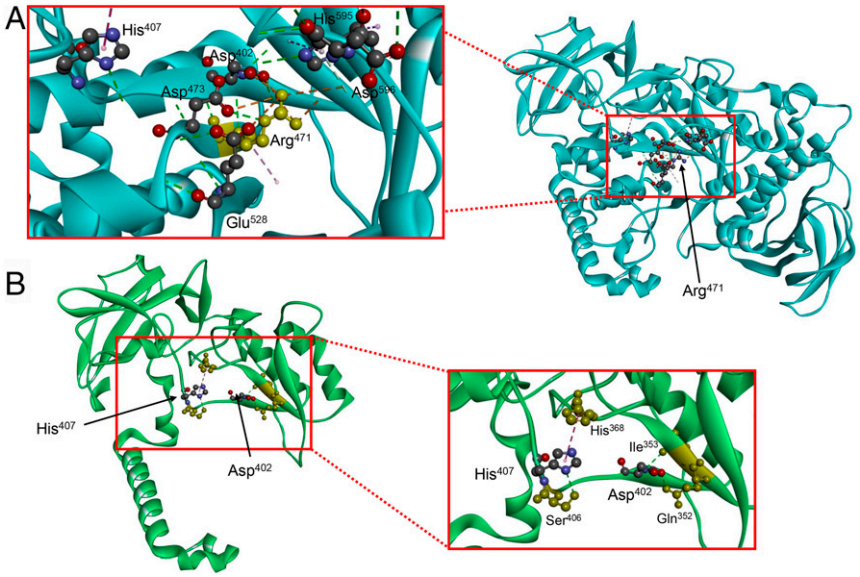

Fig. 1. Structural comparison of wild-type OsSBEIIb and the mutated version in line E15. The protein is represented as a ribbon, whereas all of the labeled residues are represented as scaled ball and stick models. (*A*) Wild-type OsSBEIIb showing the position of Arg^{471}. The *Inset* box shows all of the key amino acids in the central catalytic domain (Asp^{402}, His^{407}, Arg^{471} [yellow], Asp^{473}, Glu^{528}, His^{595}, and Asp^{596}). Dashed lines show the intramolecular interactions (orange, salt bridge; green, hydrogen bond; purple, π-interactions). (*B*) Mutant OsSBEIIb in line E15 showing the position of His^{407} and Asp^{402}. The *Inset* box shows that His^{407} has the same interactions with His^{368} and Ser^{406} as shown for the wild-type protein, but Asp^{402} no longer interacts with Arg^{471} but retains the normal interactions with Ile^{353} and Gln^{352}. Amino acids that interact with His^{407} and Asp^{402} are colored yellow. Dashed lines show the intramolecular interactions (green, hydrogen bond; purple, π-interactions).

gene was strongly down-regulated (1.8-fold) in the mutant, whereas the leaf-specific *OsGBSSII* gene was slightly down-regulated.

We observed the strong down-regulation of *OsSBEIIb* (3.5-fold) in the endosperm, possibly reflecting the direct effect of the truncated coding region on the mRNA quality control system via nonsense-mediated mRNA decay. *OsSBEIIb* was expressed at low levels in wild-type leaves, but even in this tissue we were able to detect a statistically significant down-regulation (1.5-fold) in line E15. *OsSBEI* was expressed in both tissues in wild-type plants, albeit at a higher level in the endosperm. In the mutant plants, there was no significant change in the endosperm but a significant (1.4-fold) up-regulation in the leaves. *OsSBEIIa* was mainly expressed in the leaves of wild-type plants and it was significantly (1.8-fold) up-regulated in the leaves of mutant plants, whereas there was no change in the endosperm.

The DBE genes *OsISA1–3* were expressed at low levels in the endosperm and leaves of wild-type plants, and the significant changes were the down-regulations of *OsISA1* and *OsISA3* by 1.2-fold in the leaves. The pullulanase (*OsPUL*) and plastidial starch phosphorylase (*OsPHOL*) genes were expressed more strongly in the endosperm than the leaves, but there was no significant change in the endosperm of line E15, whereas *OsPUL* expression fell by 1.6-fold and *OsPHOL* by 1.9-fold in the mutant leaves. The cytosolic starch phosphorylase (*OsPHOH*) gene, which was mainly expressed in the leaves of wild-type plants, was also significantly (1.4-fold) down-regulated in the mutant leaves (Fig. 3*B* and *SI Appendix*, Table S2).

Loss of OsSBEIIb Activity Triggers Changes in Endosperm Primary and Secondary Metabolism. Having established that the loss of OsSBEIIb activity affected the expression of all classes of starch biosynthesis enzymes in seeds and also in leaves, we extracted polar and nonpolar metabolites from the endosperm of wild-type plants and line E15 in order to compare the broader metabolic profiles. Principal component analysis (PCA) revealed clear genotype-specific differences in metabolic composition between the wild-type and two biological replicates of the mutant. The first principal component (PC1) which is related to the metabolic differences mostly in sugars, fatty acids, sterols, amino acids, organic acids, and phenols explained 73.2% of total variance among the genotypes, while PC2 explained 5.9% between the genotypes (*SI Appendix*, Fig. S4). The comparison of extracts produced by gas chromatography/mass spectrometry (GC/MS) revealed 50 metabolites in the endosperm tissue (*SI Appendix*, Table S3), of which 42 showed genotype-specific differences in the heat map (Fig. 4) and pathway analysis (Fig. 5).

Three sugars were present at significantly higher levels in the mutant endosperm compared to the wild-type plants. There was a 2-fold increase in sucrose, a 10-fold increase in glucose, and a 23-fold increase in fructose. Furthermore, glycerol–galactose was not detected in wild-type endosperm, but accumulated to a concentration of 1 mg/g in line E15. *Myo*-inositol levels were also significantly (1.8-fold) higher in the mutant. Glycerol was the only polyol present at the same concentration in both genotypes, and sedoheptulose was the only sugar that was significantly (3-fold) less abundant in the mutant.

Several fatty acids also accumulated to higher levels in the mutant. There was a 1.3-fold increase in stearic acid (C18:0), a >1.5-fold increase in myristic acid (C14:0), palmitic acid (C16:0), linoleic acid (C18:2), and behenic acid (C22:0), and a 2.6-fold increase in arachidic acid (C20:0). Furthermore, pentadecanoic acid (C15:0) was not detected in wild-type endosperm but accumulated to a concentration of >2 μg/g in line E15. The only fatty acid present at similar levels in both genotypes was lauric acid (C12:0).

Several amino acids were not detected in the wild-type endosperm (alanine, aspartic acid, glycine, lysine, proline, serine, and valine) but accumulated to detectable levels in the mutant, with alanine, aspartic acid, and proline all accumulating to levels in excess of 100 μg/g. Citric acid was also significantly (1.7-fold) more abundant in the mutant, whereas benzoic acid accumulated to similar levels in both genotypes. Gluconic acid was not detected in wild-type endosperm but the concentration was >50 μg/g in the mutant line. The concentrations of campesterol, stigmasterol, and

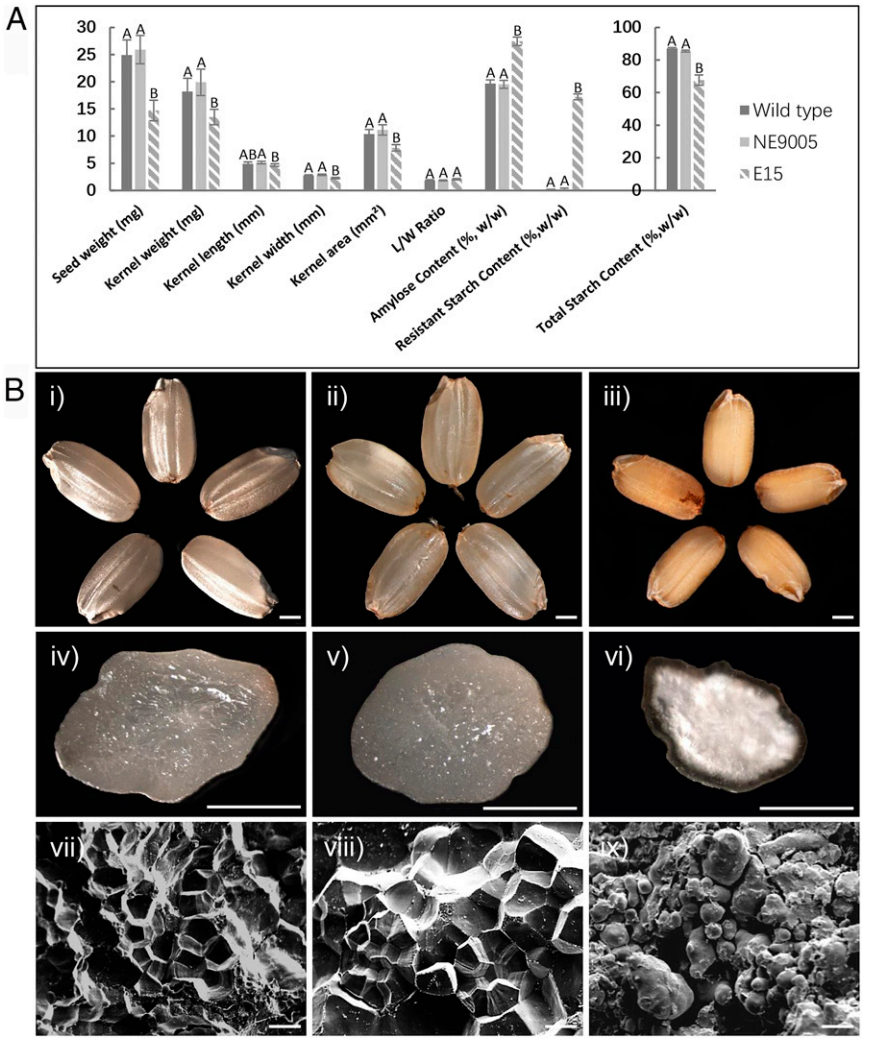

Fig. 2. Starch properties and grain morphology of wild-type rice, Tos17 insertion line NE9005, and mutant line E15. (*A*) Properties of the starch in all three genotypes. Samples annotated with different letters are significantly different from one another as determined by ANOVA ($P < 0.01$). (*B*) Gross morphology (*i–iii*) and transverse sections (*iv–vi*) of the seeds, and scanning electron microscopy images (*vii–ix*) of starch grains in the endosperm. (Scale bars, 1 mm in *i–vi*; 5 μm in *vii–ix*.)

β-sitosterol were significantly (>1.7-fold) higher in the mutant, whereas the levels of two aliphatic alcohols (dodecanol and an alkene alcohol) were similar in both genotypes, and triacontanol was 1.3-fold more abundant in line E15.

The mutant line accumulated significantly higher levels of phosphate (1.4-fold), methyl phosphate (3.8-fold, from the derivatizing agent), and glycerol 3-phosphate (3-fold), whereas the levels of α-tocopherol were similar in both genotypes.

Discussion

Plants can thrive in a changing environment due to their phenotypic plasticity, which involves the modulation of gene expression to optimize fitness (21). One facet of phenotypic plasticity is adaptive metabolism, in which plants regulate their metabolic processes in response to stress (22). Adaptive metabolism also influences the outcome of metabolic engineering because plants adjust their metabolism in response to targeted exogenous interventions such as the introduction of one or more transgenes (23–26) or the modification of endogenous genes by targeted (14, 19) or random mutagenesis (27, 28). Although the regulation of primary and secondary metabolism has been a key focus of plant science for decades, the broader impact of metabolic interventions has only been revealed since the availability of transcriptomics and metabolomics approaches for the high-throughput quantitative analysis of gene expression and small molecules.

Starch metabolism has been studied in detail because starch is the major storage carbohydrate in higher plants and is therefore the main source of carbon for all primary and secondary metabolites in storage tissues (29). However, starch also accumulates transiently in rapidly proliferating vegetative tissues, such as the cells immediately adjacent to the division zones of meristems (30). Interest in starch metabolism also reflects its importance in human nutrition and as a feedstock for industrial applications, including the production of biofuels (31). Starch accounts for up to 75% of the mass of cereal grains (32), and rice in particular is a major source of both dietary and industrial starch (33). The metabolic engineering of starch metabolism is partly driven by the health benefits of resistant starch, which has a high content of amylose and is more difficult to digest (34). Resistant starch inhibits insulin release and thus lowers the risk of diabetes, obesity, and heart disease (33, 35), and also acts as a prebiotic to support a healthy colon microbiome (36). Normal rice starch

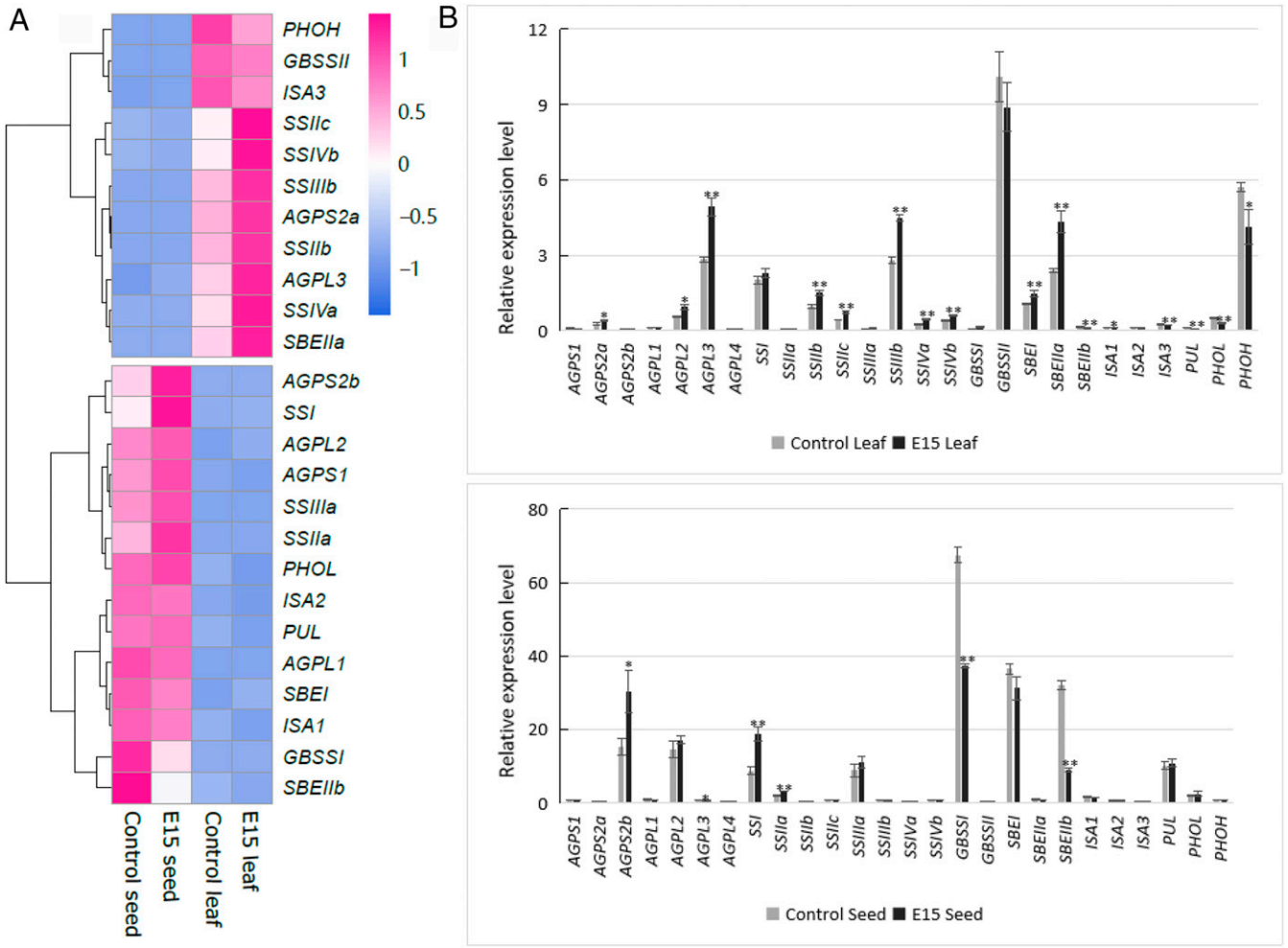

Fig. 3. Expression analysis of 26 genes representing the starch biosynthesis pathway. (*A*) Heat map summarizing the transcriptional reprogramming of the starch biosynthesis pathway in the T2 leaves and T3 seeds of line E15. Fold changes are shown in red (increase) or blue (decrease) compared to wild type. (*B*) Expression level of all 26 genes relative to *OsActin* 15 DAF in the leaves (*Top*) and seeds (*Bottom*). Each value is the mean SD of at least three independent measurements with SEs, and significant differences were determined using Student's *t* test (*$P < 0.05$, **$P < 0.01$).

consists of ~20% amylose and ~80% amylopectin (1, 2) and the content of resistant starch is typically <2% (37).

The amylose content of rice starch can be increased by suppressing the activity of OsSBEIIb, the main isoform of SBE responsible for amylopectin synthesis in the endosperm (9, 38, 39). We previously reported the mutation of *OsSBEIIb* in japonica cultivar Nipponbare using the CRISPR/Cas9 system to introduce a 4-bp deletion in exon 12, without any off-target effects, generating a truncated protein with no catalytic activity (19). Here we analyzed the T3 seeds of a homozygous mutant line (E15) and found that the amylose content was 27.4%. This was 1.4-fold higher than that of wild-type seeds (19.6%) and Tos17 insertion line NE9005 (19.5%), an additional negative control with the transposon integrated into *OsSBEIIb* intron 18. The E15 seeds also contained a much higher content of resistant starch (17.2%, compared to 0.2% in the wild-type and NE9005 seeds). This came at the expense of a ~26% fall in the total starch content and significantly lower dry seed and dehulled grain weights. Morphological analysis also revealed that the mutant seeds were opaque and the starch grains were abnormal in size, shape, and distribution.

Similar outcomes have been reported in earlier studies involving the mutation of *OsSBEIIb*. The original *ae* mutant generated by chemical mutagenesis in japonica cultivar Kinmaze increased the amylose content from 15.7 to 26.5% and the grain weight decreased by 32% (9). The knockdown of *OsSBEIIb* by hairpin RNA (RNAi) and microRNA expression in japonica cultivar Nipponbare increased the resistant starch content to 9.5% and the grain weight decreased by 30% (40). In this case, the total starch content was shown to increase (albeit by only ~1%), which together with the lower grain weight resulted in the starch representing up to 90% of the grain. Similarly, the targeted mutation of *OsSBEIIb* exon 3 in cultivar Kinmaze using CRISPR/Cas9 increased the amylose content to 25% and the resistant starch content to 9.8% while the grain weight fell by 30%, and there was a slight but statistically nonsignificant decrease in total starch (41). The simultaneous knockdown of *OsSBEIIb* and *OsSBEI* by RNAi in a high-amylose indica rice variety increased the amylose content from 27.2 to 64.8% and the resistant starch content from 0 to 14.6% while the grain weight fell by 38% (34). Finally, chemical mutagenesis in japonica cultivar Jiangtangdao increased the amylose content from 16.2 to 31.1% and the resistant starch content from 0.4 to 11.7% (37). All of these studies also reported opaque rather than translucent seeds and abnormal starch grains, in broad agreement with our results. Furthermore, the inactivation of both

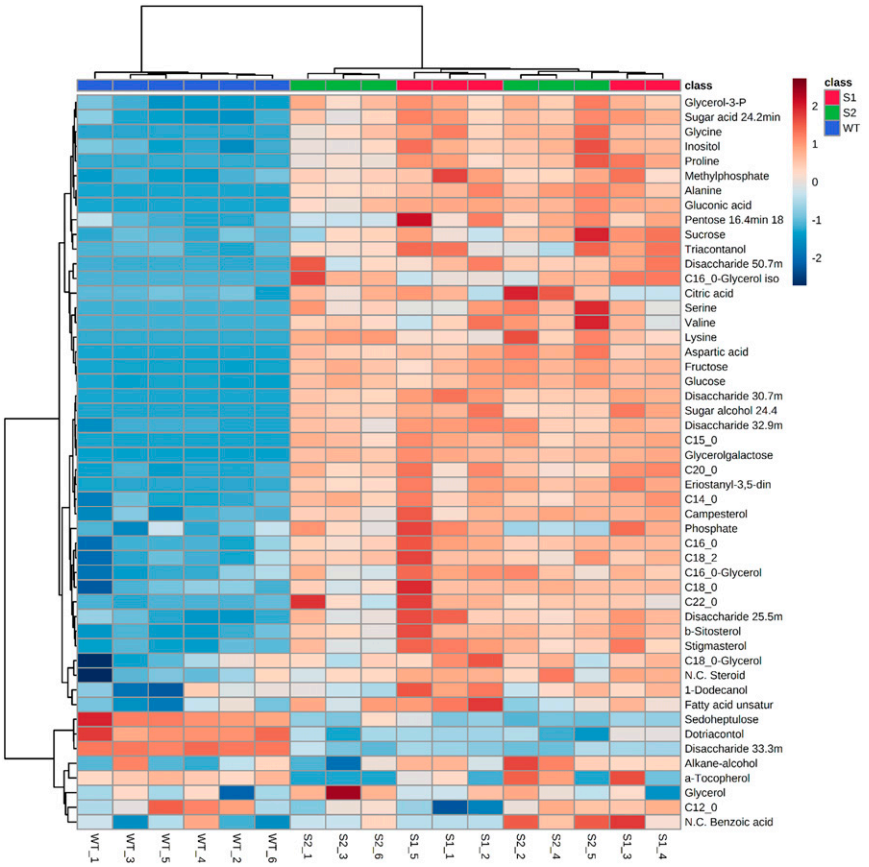

Fig. 4. Heat map of polar and nonpolar metabolites identified in rice endosperm. S1 and S2 are two biological replicates of line E15 and WT is a wild-type segregant (azygous control). Individual columns represent technical replicates of WT, S1, and S2 (*Bottom* of the plot). Fold changes are indicated by varying shades of blue (decrease) and red (increase) compared to wild-type seeds. N.C., not confirmed.

homologs of *TaSBEIIa* in a tetraploid durum wheat line increased the amylose content by 22%, whereas the inactivation of single homologs had no effect (42). The suppression of *TaSBEIIb* by RNAi in wheat had no effect on the amylose content, whereas the suppression of both *TaSBEIIa* and *TaSBEIIb* increased the amylose content to >70% (35) and similar results were reported for the barley genes *HvSBEIIa* and *HvSBEIIb* (43). Note that in wheat and barley it is the SBEIIa isoform that is predominantly active in the endosperm in contrast to the SBEIIb isoform in rice and maize.

Subtle differences in the amylose and resistant starch content of rice endosperm in the different studies discussed above may reflect the different rice cultivars used in each case, the different suppression strategies (mutation or RNAi), and the different mutation sites in *OsSBEIIb*. Starch branching enzymes comprise three domains (20, 44). The highly conserved central domain is responsible for catalytic activity, the N-terminal domain is selective for the size of the α-glucan chain, and the C-terminal domain regulates substrate preference and catalytic activity (20). Homology modeling and molecular dynamics simulations based on ZmSBEIIb indicated that phosphorylated Ser^{297} forms a salt bridge with Arg^{665} to stabilize the protein (45). Our mutation in line E15 introduces a frameshift immediately downstream of Gly^{418} thus removing Arg^{471} (which plays a key role in the stabilization of the catalytic center) as well as the catalytic triad (Asp^{473}, Glu^{528}, and Asp^{596}). Furthermore, the mutation disrupts salt bridges involving residues Ser^{323} and Arg^{691}. Finally, we observed the strong down-regulation of *OsSBEIIb* gene expression in both leaves and seeds. The mutation completely abolishes OsSBEIIb activity by a combination of removing the catalytic triad, destabilizing the entire catalytic center, abolishing important intramolecular bonds, and feeding back to suppress *OsSBEIIb* gene expression (potentially) by inducing nonsense-mediated decay.

To evaluate the broad impact of the *OsSBEIIb* mutation on starch metabolism, we selected 26 genes representing the starch biosynthesis pathway and evaluated their expression levels in the endosperm and leaves. Previous studies of *OsSBEIIb* mutants and RNAi lines have mainly concentrated on the physicochemical properties of starch and the morphology of the endosperm, but have also considered the potential impact on other aspects of the starch biosynthesis pathway by looking at selected enzyme activities and/or gene expression levels. For example, analysis of the original *ae* mutant revealed that the loss of OsSBEIIb activity had no effect on the activities of OsSBEI, OsSBEIIa, isoamylase, OsPUL, and OsSSIII, but reduced the activity of OsSSI by 50% and increased the activities of AGPase and sucrose synthase by 25% (9). Interestingly, the same study noted that while *OsSBEIIb* gene expression was down-regulated, the *OsSSI* and *OsSSIII* genes were up-regulated, which is broadly consistent with our results. We also found that *OsSSI*, *OsSSIIIa*, and *OsSSIIIb* were up-regulated in the seeds, although the increase in *OsSSIIIa* expression between wild-type and mutant plants was not statistically significant. Furthermore, the up-regulation of *OsSSI* gene expression did not correlate with the 50% loss of OsSSI activity they detected (9). However, a number of studies have shown that gene expression levels do not directly mirror changes in protein abundance or enzymatic activity (5, 46).

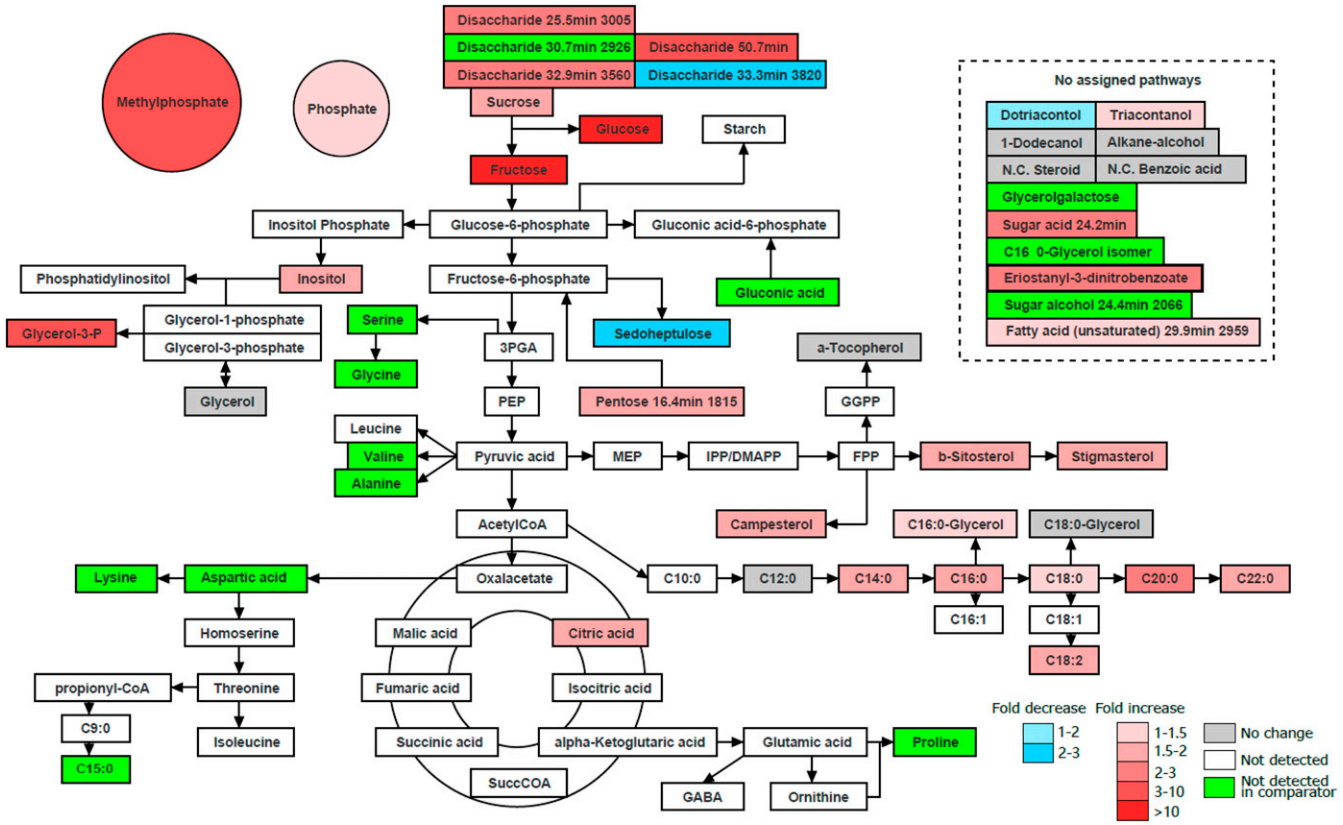

Fig. 5. Metabolic pathway highlighting significant changes in the endosperm of line E15 compared to wild-type seeds. Significant changes are shown as gradients of red (higher levels in E15), blue (lower levels in E15), and green (detected only in E15). Metabolites with the same abundance in both genotypes are shown in gray and those undetected in either genotype are shown in white. The average of six technical replicates was used for all calculations. N.C., not confirmed.

OsAGPase and OsGBSSI activity increased and OsSSI activity decreased in the triple mutant line generated by crossing the original *ae* mutant with lines carrying mutations in the *OsSSIIa* and *OsSSIIIa* genes, which Asai et al. proposed was a response to correct for the imbalance between branching and elongation in the mutant (13). The silencing of *OsSBEIIb* expression by RNAi led to the anticipated decrease in *OsSBEIIb* expression levels but did not affect the expression of *OsSBEI*, *OsSSI*, *OsSSIIa*, or *OsSSIIIa* (40) all of which except *OsSSIIIa* were up-regulated in our E15 line. In another RNAi strategy targeting *OsSBEI* and *OsSBEIIb* simultaneously, the target genes were completely suppressed at the mRNA and protein levels, but the abundance of OsGBSSI protein was unaffected. We observed the strong down-regulation of *OsGBSSI* gene expression in the seeds of line E15, although in this case it was a single mutation and we measured mRNA levels, so the two experiments are not comparable.

Although previous studies of *OsSBEIIb* mutants have only considered a small selection of genes, making direct comparisons with our study largely uninformative, a broad panel of starch biosynthesis genes was evaluated in lines generated by mutating *OsGBSSI* (14) and *OsAGPL2* (15). In both cases, the authors noted wide-ranging effects on gene expression in leaves and seeds even though the gene they targeted encoded an endosperm-specific enzyme. Also, in both cases, the response included the ectopic expression of normally compartmentalized enzymes, such as normally leaf-specific *OsGBSSII* expressed in the endosperm and normally endosperm-specific *OsAGPL2* and *OsAGPS2b* expressed in the leaves, generating an ectopic complete AGPase in the leaf cytosol. These phenomena highlight the complex responses that may follow metabolic interventions due to adaptive metabolism (22). We followed a similar strategy by evaluating 26 genes representing five classes of enzymes. We used seeds harvested at 15 DAF, representing the midpoint of starch accumulation in developing rice grains (5, 47), and leaf tissue harvested at the same time.

The first set of genes encoded components of AGPase. We found that *OsAGPS2b* and *OsAGPL3* were significantly up-regulated in the mutant seeds (although the latter was expressed at minimal levels) whereas *OsAGPS2a*, *OsAGPL2*, and *OsAGPL3* were significantly up-regulated in the mutant leaves. The other genes were either not expressed at this stage or there was no significant difference between wild-type and mutant plants. In addition to amylopectin, AGPase is also required for amylose synthesis (providing a substrate for SBEs) so there is potential for feedback inhibition if the loss of OsSBEIIb activity causes the accumulation of amylose. However, the response we observed was positive rather than negative, suggesting a more complex regulatory interaction. Complex responses have been reported in earlier studies, where the mutation of one AGPase isoform results in compensatory changes among the others, including unanticipated ectopic expression profiles (5, 15). The second set of genes encoded starch synthases, which elongate α-polyglucan chains. SSI elongates shorter chains than the various isoforms of SSII, SSIII, and SSIV (48). We found that the expression of all detectable soluble SS isoforms was up-regulated in line E15 (*OsSSI* and *OsSSIIa* in the endosperm and *OsSSIIb*/*c*, *OsSSIIIb*, and *OsSSIVa*/*b* in the leaves). This may reflect the greater availability of longer α-polyglucan chains, which have been shown to bind SSI with greater affinity than shorter segments (48). The only starch synthase gene that was down-regulated in

the mutant was *OsGBSSI* (*Waxy*), which catalyzes the extension of long glucan chains primarily in amylose (49). The enzyme is restricted to starch grains, and the depletion of this enzyme may explain the abnormal morphology we observed. The third group of genes encoded SBEs. As discussed above, *OsSBEIIb* expression was significantly down-regulated, reflecting a combination of feedback mechanisms and, potentially, nonsense-mediated decay. *OsSBEI* expression in the endosperm was not significantly affected by the mutation, but both *OsSBEI* and *OsSBEIIa* (the main SBE isoform in the leaf) were up-regulated in leaf tissue, suggesting this is a direct compensatory change in response to the mutation. In maize, the lack of ZmSBEIIb can be partially complemented by ZmSBEIIa and ZmSBEI (50). The remaining genes encoded DBEs, PUL, PHOL, and PHOH, which degrade starch and/or modify excessively or incorrectly branched chains (5). The main role of SBEIIb in rice is to introduce new branches into α-polyglucans, so the loss of this enzyme reduces the need for DBEs, PUL, PHOL, and PHOH by removing many of their substrates. This may explain the suppression of the corresponding genes in the leaves of line E15.

The full impact of metabolic interventions can only be determined by metabolomic analysis, and we therefore carried out a broad survey of the endosperm metabolome to identify genotype-specific differences in the content of polar and nonpolar metabolites. We anticipated changes in carbohydrate metabolism, which is directly linked to the synthesis of starch, but also evaluated the broader metabolic landscape to look for ripple effects caused by the spillover of intermediates into other pathways and/or the disruption of enzyme complexes. Protein–protein interactions between enzymes in the starch biosynthesis pathway have been demonstrated in rice (16), wheat (51, 52), maize (50, 53–55), and barley (56), and the resulting complexes may also include enzymes from linked pathways that regulate carbon partitioning between starch and lipids (53). The starch biosynthesis pathway also differs in source and sink tissues because the carbon is derived from fructose-6-phosphate (Calvin–Benson cycle) in source tissues but from sucrose (transported via the phloem) in sink tissues (5). The sucrose must then be phosphorylated or converted to ADP-glucose in the cytoplasm and translocated into the amyloplasts via the compound-specific hexose monophosphate translocator or the ADP-glucose translocator, respectively (48).

One of the key metabolic effects in line E15 was the greater abundance of soluble sugars, which is a direct result of the ∼26% reduction in starch levels. Similar effects have been reported for other starch biosynthesis mutants in rice (14, 15, 57). The sucrose level in the mutant was twice that in wild-type endosperm, but the amount of glucose and fructose was 10 to 20 times higher. This may reflect the balance of sucrose hydrolysis vs. amylose synthesis in the endosperm, combined with the strong down-regulation of *OsGBSSI*, which encodes the only enzyme that transfers glucosyl units from ADP-glucose and utilizes soluble malto-oligosaccharides as a substrate for amylose production (31). Only sedoheptulose was significantly depleted in the mutant, probably reflecting the diversion of fructose-6-phosphate toward the synthesis of pyruvic acid, acetyl-CoA, and oxaloacetate for the synthesis of additional metabolites, as discussed below (Fig. 5). The disruption of the normal metabolic balance between starch and soluble sugars is also likely to affect the activity of AGPases and the availability of ADP-glucose and pyrophosphate, which in turn may explain the higher inorganic phosphate levels we observed in the E15 endosperm.

Another notable metabolic effect in line E15 was the greater abundance of fatty acids. The dosage effect of *ae* mutants affects the fatty acid content as well as the starch content of maize seeds (58) and there is strong evidence that amylose and lipid biosynthesis are interdependent (59, 60). This is because both products compete for the same precursors during grain filling, so any deficiency in the starch biosynthesis pathway is likely to provide the lipid pathway with additional substrates (61). For example, starch deficiency in *Arabidopsis thaliana* resulted in the accumulation of sugars and significantly increased fatty acid synthesis via the modulation of acetyl-CoA carboxylase activity (62). The down-regulation of AGPase also increased fatty acid accumulation in sugarcane and potato (63, 64). In the rice *floury shrunken endosperm 1* (*fse1*) mutant, the reduction in total starch and amylose levels was complemented by a ∼48% increase in total lipids (65). The ∼26% loss of total starch in line E15 is therefore consistent with the increase in fatty acid levels, although the levels of lauric acid (C12:0) remained stable, perhaps because amylose can form complexes with longer-chain fatty acids (66).

We also observed a strong increase in the levels of multiple amino acids and phytosterols, indicating the profound redirection of metabolic flux as a means of carbon partitioning in the endosperm (48). This appears to reflect the greater abundance of sucrose, glucose, and fructose, which feed directly or indirectly into the glycolytic pathway, yielding higher quantities of glucose-6-phosphate (diverted to inositol biosynthesis), 3-phosphoglycerate (diverted to the synthesis of serine and glycine), pyruvate (diverted to the synthesis of valine and alanine, and also into the MEP pathway), acetyl-CoA (utilized for the synthesis of fatty acids), oxaloacetate (utilized for the synthesis of aspartic acid and lysine), and the remaining citric acid cycle organic acids (leading to the synthesis of proline). Environmental factors that affect core metabolism in rice have previously been shown to modulate the synthesis of amino acids and other nitrogen-rich compounds such as polyamines (67) and serotonin (68), and the utilization of excess sugars to fuel nitrogen metabolism has been reported in other starch mutants (69).

In conclusion, we found that mutating the *OsSBEIIb* gene in line E15 caused the complete inactivation of the enzyme OsSBEIIb and resulted in the accumulation of amylose-rich resistant starch, although the total starch content of the grains fell by ∼26%. This triggered the broad transcriptional reprogramming of starch metabolism, up-regulating the expression of several AGPase subunits and genes encoding soluble SS and SBE, but suppressing the expression of *OsGBSSI* and multiple genes encoding DBEs and disproportionating enzymes. These responses are broadly in line with earlier reports and reflect the adjustment of metabolism to deal with the higher levels of amylose and lower levels of amylopectin. More broadly, the release of sucrose, glucose, and fructose resulted in the profound redirection of flux through core metabolism (glycolysis and the citric acid cycle) boosting the synthesis of multiple fatty acids and amino acids, as well as secondary products of the MEP pathway (phytosterols) and additional products such as gluconic acid, glycerol–galactose, and triacontanol. Our results provide insight into the broader implications of perturbing starch metabolism in rice endosperm and its impact on the whole plant, which will make it easier to predict the effect of metabolic engineering in cereals for nutritional improvement or the production of valuable metabolites.

Materials and Methods

A detailed description of the materials and methods and all statistical treatments is given in *SI Appendix, Materials and Methods*.

Plant Material. A homozygous *OsSBEIIb* mutant rice line (*Oryza sativa* cv Nipponbare) generated previously using the CRISPR/Cas9 system and a Tos17 insertion line (NE9005) from the Rice Tos17 Insertion Mutant Database were used (19).

Gene Expression Analysis by Quantitative Real-Time PCR. Total RNA was isolated from T2 leaf and T3 endosperm tissue using the RNeasy Plant Mini Kit

(Qiagen) as described in detail in *SI Appendix*. Quantitative real-time RT-PCR (qRT-PCR) was carried out as previously described (70) using the gene-specific primers listed in *SI Appendix*, Table S4. The identity of the PCR products was confirmed by sequencing.

Homology Modeling and Protein Structure Analysis. Automated homology modeling was carried out using Phyre2 (71) as described in *SI Appendix*.

Amylose and Resistant Starch Content. The relative amylose content of whole-grain flour was determined using the AMYLOSE/AMYLOPECTIN kit (Megazyme International) according to the manufacturer's instructions. The resistant starch content was determined using the RESISTANT STARCH kit (Megazyme International, AOAC Official Method 2002.02 and AACC Method 32-40.01).

Light Microscopy and Scanning Electron Microscopy. A Leica MZ8 stereo microscope coupled to a Leica DFC digital camera were used for light microscopy. The morphology of starch grains was observed by scanning electron microscopy. Images were captured using a JEOL JSM-6360LV instrument.

Metabolite Analysis and Identification. Metabolites in freeze-dried rice seeds were identified by GC/MS analysis based on their retention times, retention indices, and mass spectra, and the area quantified relative to the internal standards (please see *SI Appendix* annex).

Data Analysis and Statistical Tests. A one-way analysis of variance (ANOVA) was used in determining differences in grain morphology and starch physiochemical properties. For metabolomic datasets, PCA was applied after autoscaling using MetaboAnalyst v4.0 (72).

Data Availability. All study data are included in the article and *SI Appendix*.

ACKNOWLEDGMENTS. We would like to acknowledge funding from Ministry of Economy and Competitiveness, Spain (RTI2018-097613-BI00 to C.Z., PGC2018-097655-B-I00 to P.C., and AGL2017-85377-R to T.C.); Generalitat de Catalunya Grant 2017 SGR 828 to the Agricultural Biotechnology and Bioeconomy Unit; and the European Union Framework Program DISCO (from discovery to final products: a next-generation pipeline for the sustainable generation of high-value plant products; Project 613513) to P.D.F. We are grateful to Dr. A. Miyao and Dr. Y. Katayose (Rice Genome Research Center, Institute of Crop Science, National Agriculture and Food Research Organization) for providing the rice Tos17 insertion mutant seeds.

1. I. J. Tetlow, Starch biosynthesis in developing seeds. *Seed Sci. Res.* **21**, 5–32 (2010).
2. N. Crofts *et al*., Amylopectin biosynthetic enzymes from developing rice seed form enzymatically active protein complexes. *J. Exp. Bot.* **66**, 4469–4482 (2015).
3. Z. Tian *et al*., Allelic diversities in rice starch biosynthesis lead to a diverse array of rice eating and cooking qualities. *Proc. Natl. Acad. Sci. U.S.A.* **106**, 21760–21765 (2009).
4. J. Qu *et al*., Evolutionary, structural and expression analysis of core genes involved in starch synthesis. *Sci. Rep.* **8**, 12736 (2018).
5. T. Ohdan *et al*., Expression profiling of genes involved in starch synthesis in sink and source organs of rice. *J. Exp. Bot.* **56**, 3229–3244 (2005).
6. Y. Nakamura, Towards a better understanding of the metabolic system for amylopectin biosynthesis in plants: Rice endosperm as a model tissue. *Plant Cell Physiol.* **43**, 718–725 (2002).
7. H. Satoh *et al*., Isolation and characterization of starch mutants in rice. *J. Appl. Glycosci.* **50**, 225–230 (2003).
8. Y. Nakamura *et al*., Characterization of the reactions of starch branching enzymes from rice endosperm. *Plant Cell Physiol.* **51**, 776–794 (2010).
9. A. Nishi, Y. Nakamura, N. Tanaka, H. Satoh, Biochemical and genetic analysis of the effects of amylose-extender mutation in rice endosperm. *Plant Physiol.* **127**, 459–472 (2001).
10. H. Satoh *et al*., Starch-branching enzyme I-deficient mutation specifically affects the structure and properties of starch in rice endosperm. *Plant Physiol.* **133**, 1111–1121 (2003).
11. N. Abe *et al*., Relationships between starch synthase I and branching enzyme isozymes determined using double mutant rice lines. *BMC Plant Biol.* **14**, 80 (2014).
12. T. Sawada, M. Itoh, Y. Nakamura, Contributions of three starch branching enzyme isozymes to the fine structure of amylopectin in rice endosperm. *Front. Plant Sci.* **9**, 1536 (2018).
13. H. Asai *et al*., Deficiencies in both starch synthase IIIa and branching enzyme IIb lead to a significant increase in amylose in SSIIa-inactive japonica rice seeds. *J. Exp. Bot.* **65**, 5497–5507 (2014).
14. L. Pérez *et al*., CRISPR/Cas9 mutations in the rice Waxy/GBSSI gene induce allele-specific and zygosity-dependent feedback effects on endosperm starch biosynthesis. *Plant Cell Rep.* **38**, 417–433 (2019).
15. L. Pérez *et al*., CRISPR/Cas9-induced monoallelic mutations in the cytosolic AGPase large subunit gene APL2 induce the ectopic expression of APL2 and the corresponding small subunit gene APS2b in rice leaves. *Transgenic Res.* **27**, 423–439 (2018).
16. N. Crofts *et al*., Rice mutants lacking starch synthase I or branching enzyme IIb activity altered starch biosynthetic protein complexes. *Front. Plant Sci.* **9**, 1817 (2018).
17. M. Decourcelle *et al*., Combined transcript, proteome, and metabolite analysis of transgenic maize seeds engineered for enhanced carotenoid synthesis reveals pleotropic effects in core metabolism. *J. Exp. Bot.* **66**, 3141–3150 (2015).
18. M. Galland *et al*., An Integrated "Multi-Omics" Comparison of embryo and endosperm tissue-specific features and their impact on rice seed quality. *Front. Plant Sci.* **8**, 1984 (2017).
19. C. Baysal *et al*., CRISPR/Cas9 activity in the rice OsBEIIb gene does not induce off-target effects in the closely related paralog OsBEIIa. *Mol. Breed.* **36**, 108 (2016).
20. I. J. Tetlow, M. J. Emes, A review of starch-branching enzymes and their role in amylopectin biosynthesis. *IUBMB Life* **66**, 546–558 (2014).
21. S. Matesanz, E. Gianoli, F. Valladares, Global change and the evolution of phenotypic plasticity in plants. *Ann. N. Y. Acad. Sci.* **1206**, 35–55 (2010).
22. L. Shaar-Moshe, R. Hayouka, U. Roessner, Z. Peleg, Phenotypic and metabolic plasticity shapes life-history strategies under combinations of abiotic stresses. *Plant Direct* **3**, e00113 (2019).
23. T. Capell, L. Bassie, P. Christou, Modulation of the polyamine biosynthetic pathway in transgenic rice confers tolerance to drought stress. *Proc. Natl. Acad. Sci. U.S.A.* **101**, 9909–9914 (2004).
24. S. Naqvi *et al*., Transgenic multivitamin corn through biofortification of endosperm with three vitamins representing three distinct metabolic pathways. *Proc. Natl. Acad. Sci. U.S.A.* **106**, 7762–7767 (2009).
25. C. Zhu *et al*., Combinatorial genetic transformation generates a library of metabolic phenotypes for the carotenoid pathway in maize. *Proc. Natl. Acad. Sci. U.S.A.* **105**, 18232–18237 (2008).
26. E. Vamvaka *et al*., Unexpected synergistic HIV neutralization by a triple microbicide produced in rice endosperm. *Proc. Natl. Acad. Sci. U.S.A.* **115**, E7854–E7862 (2018).
27. J.-L. Wu *et al*., Chemical- and irradiation-induced mutants of indica rice IR64 for forward and reverse genetics. *Plant Mol. Biol.* **59**, 85–97 (2005).
28. M. A. J. Parry *et al*., Mutation discovery for crop improvement. *J. Exp. Bot.* **60**, 2817–2825 (2009).
29. M. V. Busi *et al*., "Starch metabolism in green plants" in *Polysaccharides*, K. Ramawat, J. M. Mérillon, Eds. (Springer, Cham, 2015), pp. 329–376.
30. M. N. Jordy, Seasonal variation of organogenetic activity and reserves allocation in the shoot apex of Pinus pinaster Ait. *Ann. Bot.* **93**, 25–37 (2004).
31. S. C. Zeeman, J. Kossmann, A. M. Smith, Starch: Its metabolism, evolution, and biotechnological modification in plants. *Annu. Rev. Plant Biol.* **61**, 209–234 (2010).
32. W. Laskowski, H. Górska-Warsewicz, K. Rejman, M. Czeczotko, J. Zwolińska, How important are cereals and cereal products in the average Polish diet? *Nutrients* **11**, 679 (2019).
33. R. L. Ordonio, M. Matsuoka, Increasing resistant starch content in rice for better consumer health. *Proc. Natl. Acad. Sci. U.S.A.* **113**, 12616–12618 (2016).
34. L. Zhu *et al*., High-amylose rice improves indices of animal health in normal and diabetic rats. *Plant Biotechnol. J.* **10**, 353–362 (2012).
35. A. Regina *et al*., High-amylose wheat generated by RNA interference improves indices of large-bowel health in rats. *Proc. Natl. Acad. Sci. U.S.A.* **103**, 3546–3551 (2006).
36. X. Yang *et al*., Resistant starch regulates gut microbiota: Structure, biochemistry and cell signalling. *Cell. Physiol. Biochem.* **42**, 306–318 (2017).
37. R. Yang *et al*., A putative gene sbe3-rs for resistant starch mutated from SBE3 for starch branching enzyme in rice (Oryza sativa L.). *PLoS One* **7**, e43026 (2012).
38. N. Tanaka *et al*., The structure of starch can be manipulated by changing the expression levels of starch branching enzyme IIb in rice endosperm. *Plant Biotechnol. J.* **2**, 507–516 (2004).
39. T. Sawada *et al*., Chlorella starch branching enzyme II (BEII) can complement the function of BEIIb in rice endosperm. *Plant Cell Physiol.* **50**, 1062–1074 (2009).
40. V. M. Butardo *et al*., Impact of down-regulation of starch branching enzyme IIb in rice by artificial microRNA- and hairpin RNA-mediated RNA silencing. *J. Exp. Bot.* **62**, 4927–4941 (2011).
41. Y. Sun *et al*., Generation of high-amylose rice through CRISPR/Cas9-mediated targeted mutagenesis of starch branching enzymes. *Front. Plant Sci.* **8**, 298 (2017).
42. B. Hazard *et al*., Induced mutations in the starch branching enzyme II (SBEII) genes increase amylose and resistant starch content in durum wheat. *Crop Sci.* **52**, 1754–1766 (2012).
43. A. Regina *et al*., Control of starch branching in barley defined through differential RNAi suppression of starch branching enzyme IIa and IIb. *J. Exp. Bot.* **61**, 1469–1482 (2010).
44. E. A. MacGregor, S. Janecek, B. Svensson, Relationship of sequence and structure to specificity in the alpha-amylase family of enzymes. *Biochim. Biophys. Acta* **1546**, 1–20 (2001).
45. A. Makhmoudova *et al*., Identification of multiple phosphorylation sites on maize endosperm starch branching enzyme IIb, a key enzyme in amylopectin biosynthesis. *J. Biol. Chem.* **289**, 9233–9246 (2014).
46. P. Geigenberger, Regulation of starch biosynthesis in response to a fluctuating environment. *Plant Physiol.* **155**, 1566–1577 (2011).
47. S. B. Xu *et al*., Dynamic proteomic analysis reveals a switch between central carbon metabolism and alcoholic fermentation in rice filling grains. *Plant Physiol.* **148**, 908–925 (2008).
48. M. G. James, K. Denyer, A. M. Myers, Starch synthesis in the cereal endosperm. *Curr. Opin. Plant Biol.* **6**, 215–222 (2003).

49. M. L. Maddelein *et al*., Toward an understanding of the biogenesis of the starch granule. Determination of granule-bound and soluble starch synthase functions in amylopectin synthesis. *J. Biol. Chem.* **269**, 25150–25157 (1994).
50. F. Liu *et al*., The amylose extender mutant of maize conditions novel protein-protein interactions between starch biosynthetic enzymes in amyloplasts. *J. Exp. Bot.* **60**, 4423–4440 (2009).
51. I. J. Tetlow *et al*., Protein phosphorylation in amyloplasts regulates starch branching enzyme activity and protein-protein interactions. *Plant Cell* **16**, 694–708 (2004).
52. I. J. Tetlow *et al*., Analysis of protein complexes in wheat amyloplasts reveals functional interactions among starch biosynthetic enzymes. *Plant Physiol.* **146**, 1878–1891 (2008).
53. T. A. Hennen-Bierwagen *et al*., Proteins from multiple metabolic pathways associate with starch biosynthetic enzymes in high molecular weight complexes: A model for regulation of carbon allocation in maize amyloplasts. *Plant Physiol.* **149**, 1541–1559 (2009).
54. F. Liu *et al*., Allelic variants of the amylose extender mutation of maize demonstrate phenotypic variation in starch structure resulting from modified protein-protein interactions. *J. Exp. Bot.* **63**, 1167–1183 (2012).
55. F. Liu *et al*., Glucan affinity of starch synthase IIa determines binding of starch synthase I and starch-branching enzyme IIb to starch granules. *Biochem. J.* **448**, 373–387 (2012).
56. Z. Ahmed, I. J. Tetlow, R. Ahmed, M. K. Morell, M. J. Emes, Protein-protein interactions among enzymes of starch biosynthesis in high-amylose barley genotypes reveal differential roles of heteromeric enzyme complexes in the synthesis of A and B granules. *Plant Sci.* **233**, 95–106 (2015).
57. X. J. Tang *et al*., ADP-glucose pyrophosphorylase large subunit 2 is essential for storage substance accumulation and subunit interactions in rice endosperm. *Plant Sci.* **249**, 70–83 (2016).
58. J. South, W. Morrison, O. Nelson, A relationship between the amylose and lipid contents of starches from various mutants for amylose in maize. *J. Cereal Sci.* **4**, 267–268 (1991).
59. W. R. Morrison, R. V. Law, C. E. Snape, Evidence for inclusion complexes of lipids with V-amylose in maize, rices and oat starches. *J. Cereal Sci.* **18**, 107–109 (1993).
60. V. K. Villwock, A. C. Eliasson, J. Silverio, J. N. BeMiller, Starch-lipid interactions in common, waxy, ae du, and ae su2 maize starches examined by differential scanning calorimetry 1. *Cereal Chem.* **76**, 292–298 (1999).
61. H. G. Kang, S. Park, M. Matsuoka, G. An, White-core endosperm floury endosperm-4 in rice is generated by knockout mutations in the C-type pyruvate orthophosphate dikinase gene (OsPPDKB). *Plant J.* **42**, 901–911 (2005).
62. L. Yu, J. Fan, C. Yan, C. Xu, Starch deficiency enhances lipid biosynthesis and turnover in leaves. *Plant Physiol.* **178**, 118–129 (2018).
63. J. Zale *et al*., Metabolic engineering of sugarcane to accumulate energy-dense triacylglycerols in vegetative biomass. *Plant Biotechnol. J.* **14**, 661–669 (2016).
64. X. Xu *et al*., Upregulated lipid biosynthesis at the expense of starch production in potato (Solanum tuberosum) vegetative tissues via simultaneous downregulation of ADP-Glucose Pyrophosphorylase and Sugar Dependent1 expressions. *Front. Plant Sci.* **10**, 1444 (2019).
65. W. Long *et al*., Floury shrunken endosperm I connects phospholipid metabolism and amyloplast development in rice. *Plant Physiol.* **177**, 698–712 (2018).
66. J. Blazek, E. P. Gilbert, L. Copeland, Effects of monoglycerides on pasting properties of wheat starch after repeated heating and cooling. *J. Cereal Sci.* **54**, 151–159 (2011).
67. U. Glaubitz, A. Erban, J. Kopka, D. K. Hincha, E. Zuther, High night temperature strongly impacts TCA cycle, amino acid and polyamine biosynthetic pathways in rice in a sensitivity-dependent manner. *J. Exp. Bot.* **66**, 6385–6397 (2015).
68. P. Gupta, B. De, Metabolomics analysis of rice responses to salinity stress revealed elevation of serotonin, and gentisic acid levels in leaves of tolerant varieties. *Plant Signal. Behav.* **12**, e1335845 (2017).
69. M. Kumari, B. Asthir, Transformation of sucrose to starch and protein in rice leaves and grains under two establishment methods. *Rice Sci.* **23**, 255–265 (2016).
70. X. Jin *et al*., The subcellular localization of two isopentenyl diphosphate isomerases in rice suggests a role for the endoplasmic reticulum in isoprenoid biosynthesis. *Plant Cell Rep.* **39**, 119–133 (2020).
71. L. A. Kelley, S. Mezulis, C. M. Yates, M. N. Wass, M. J. Sternberg, The Phyre2 web portal for protein modeling, prediction and analysis. *Nat. Protoc.* **10**, 845–858 (2015).
72. J. Xia, D. S. Wishart, Using MetaboAnalyst 3.0 for comprehensive metabolomics data analysis. *Curr. Protoc. Bioinformatics* **55**, 14.10.1-14.10.91 (2016).